

Article

Coordinated Economic Operation of Hydrothermal Units with HVDC Link Based on Lagrange Multipliers

Ali Ahmad ^{1,2}, Syed Abdul Rahman Kashif ², Arslan Ashraf ¹, Muhammad Majid Gulzar ^{3,4},
Mohammed Alqahtani ⁵ and Muhammad Khalid ^{4,6,7,*}

- ¹ Department of Electrical Engineering, University of Central Punjab, Lahore 54000, Pakistan
² Department of Electrical Engineering, University of Engineering and Technology, Lahore 54890, Pakistan
³ Department of Control & Instrumentation Engineering, King Fahd University of Petroleum & Minerals, Dhahran 31261, Saudi Arabia
⁴ Interdisciplinary Research Center for Renewable Energy and Power Systems (IRC-REPS), King Fahd University of Petroleum & Minerals, Dhahran 31261, Saudi Arabia
⁵ Department of Industrial Engineering, King Khalid University, Abha 62529, Saudi Arabia
⁶ Electrical Engineering Department, King Fahd University of Petroleum & Minerals, Dhahran 31261, Saudi Arabia
⁷ SDAIA-KFUPM Joint Research Center for Artificial Intelligence, King Fahd University of Petroleum & Minerals, Dhahran 31261, Saudi Arabia
* Correspondence: mkhalid@kfupm.edu.sa

Abstract: Coordinated operation of hydrothermal scheduling with HVDC links considering network constraints becomes a vital issue due to their remote location and recent induction in the existing power system. The nonlinear and complex nature of the problem introduces many variables and constraints which results in a heavy computational burden. A widespread approach for handling these complexities is to reformulate the problem by several linearization methods. In this paper, a Lagrange multipliers-based method is proposed for the solution of hydrothermal economic scheduling including HVDC link. This method solves equality constraint optimization problems. The linear programming approach is embedded with the Lagrange method to consider both equality and inequality constraints. The proposed technique has been used on piecewise linear variables and constraints of the system considering generation, water volume, and line power flow limits. The formulated method efficiently minimizes the operational cost of thermal units and maximizes the utilization of hydro units while meeting all generation, water volume, and the HVDC link constraints. The method was successfully implemented in two scenarios of a case study. In the first scenario, hydrothermal scheduling was performed on the typical network without an HVDC line limit and equal nodal prices were found with minimal thermal generation cost of \$278,822.3. In the second scenario, the proposed method optimally dispatches units to meet the HVDC line limit and minimizes thermal generation cost to \$279,025.4 while satisfying hydro, thermal, and other operating constraints. Both scenarios are implemented for a 24 h period. The results have been presented to illustrate the performance of the proposed method.

Keywords: linear programming; economic dispatch; hydrothermal scheduling; HVDC link; Lagrange multipliers; optimal power flow

MSC: 49-11



Citation: Ahmad, A.; Kashif, S.A.R.; Ashraf, A.; Gulzar, M.M.; Alqahtani, M.; Khalid, M. Coordinated Economic Operation of Hydrothermal Units with HVDC Link Based on Lagrange Multipliers. *Mathematics* **2023**, *11*, 1610. <https://doi.org/10.3390/math11071610>

Academic Editors: Atanda Raji and Khaled M. Abo-Al-Ez

Received: 25 February 2023

Revised: 15 March 2023

Accepted: 22 March 2023

Published: 27 March 2023



Copyright: © 2023 by the authors. Licensee MDPI, Basel, Switzerland. This article is an open access article distributed under the terms and conditions of the Creative Commons Attribution (CC BY) license (<https://creativecommons.org/licenses/by/4.0/>).

1. Introduction

Recently, an increase in energy demand and fossil fuel prices has raised the cost of energy generated by thermal power plants. The world has reduced the use of costly and inefficient thermal plants by inducting renewable energy resources and hydel power generation [1,2]. The energy prices can also be minimized by optimal scheduling of

resources [3,4]. Conventionally, power is transmitted to loads through AC transmission lines. However for long distance, the HVDC link becomes more efficient and cost effective as compared to the conventional mode of transmission [5]. Therefore, the coordinated economical operation of hydrothermal units with HVDC links has emerged as an interesting research area in today's world of increasing energy stress.

Different researchers have discussed different aspects of hydrothermal scheduling considering HVDC systems. Hydrothermal scheduling is a complex and non-linear constrained optimization problem. Inclusion of HVDC links increases the complexity of the problem that can be addressed by good computational tools. Hydrothermal scheduling problems were successfully solved using conventional methods such as Lagrange multipliers method (LMM) [6], Newton–Raphson method [7,8], gradient search algorithm [9], mixed integer programming [10], and dynamic programming [11]. A number of heuristic and metaheuristic algorithms are used to solve hydrothermal scheduling problems [12–14]. A few recently used algorithms in hydrothermal scheduling operation are rigid cuckoo search algorithm [15], firefly and accelerated particle swarm optimization [16], Lagrangian relaxation [13], grasshopper optimization algorithm (GOA) [17], and artificial bee colony algorithm [18]. However, heuristic algorithms cannot deal effectively with premature convergence problems. Additionally, when dealing with the large number of variables in optimization, the computation time of heuristic algorithms increases drastically. Each metaheuristic technique has some weaknesses and strengths to find near the optimal solutions for hydrothermal scheduling [19]. Meanwhile, mathematical programming methods are computationally fast and provide stable solution each time [20]. In unit commitment and economic dispatch cases, the linear programming (LP) method gives better results than the genetic algorithm (GA) technique [21]. The literature shows that hydrothermal scheduling has been effectively performed by the Lagrange multipliers method [6,22].

The induction of HVDC links in the existing power system requires an optimal power flow (OPF) study for realistic hydrothermal scheduling. Formulation and implementation of HVDC systems for OPF has been performed in reference [23]. Combined economic operation of point-to-point VSC-HVDC and AC grids is also performed based on Lagrange multipliers efficiently [24]. Joint operation of two area HVDC links has been performed in reference [20] to improve the operational economy and efficiency. Optimal scheduling of fixed head hydrothermal scheduling considering wind uncertainty is conducted in [25]. The literature survey signifies that hydrothermal scheduling was performed using various optimization techniques under various operating conditions to minimize the fuel price of thermal units.

A careful review of the above-mentioned excellent research shows that the existing methods of the economical scheduling of hydrothermal power plants only consider the price minimization of thermal units subject to meeting the load, losses, and water discharge constraints. These calculations ignore the network details and result in snubbing effects of transmission branch loading and bus voltages [9]. Therefore, economical hydrothermal dispatching does have an important effect on line flows, and under HVDC line constraints, these effects need to be taken into account.

The main contributions of this research are:

- Formulation of complex hydrothermal scheduling problem.
- Modelling of AC grids to add network constraints using DC optimal power flow (DCOPF) in the existing scheduling problem.
- Induction of HVDC link with line flows limitation constraints in hydrothermal problem.
- Linearization of quadratic cost curves of thermal generators to deal with inequality constraints.
- Implementation of linear programming-based Lagrange multipliers methods on a case study to check the robustness of the proposed method.

In this paper, a novel hydrothermal scheduling problem with an HVDC link is formulated to meet the load demand and network constraints. The formulation is general

and allows to find out the economic impact of HVDC link power usage on hydrothermal-based AC system. An algorithm is developed to solve such a diverse problem using linear programming-based Lagrange multipliers method as it is fast and less prone to convergence issues and more deterministic in nature as compared to existing popular metaheuristic algorithms. To the best knowledge of the authors, such a coordinated economic operation of hydrothermal units with HVDC links keeping in view the power network constraints has not been discussed before.

The rest of the paper is arranged as follows. Section 2 presents the detailed formulation of the concerned problem and proposes the solution methodology. Section 3 explains the proposed research methodology for a case study of a power system. Section 4 demonstrates the results of the case study under two different scenarios to validate the effectiveness of the proposed methodology. Section 5 concludes the discussion and presents some points for future work.

2. Problem Formulation

The coordinated economic operation of hydrothermal units with HVDC link aims to minimize the operating cost of thermal units while maximizing the utilization of available reservoir water volume, fulfilling the HVDC line flow limits and satisfying the load power balance. Figure 1 shows the generalized network diagram considered for this scenario.

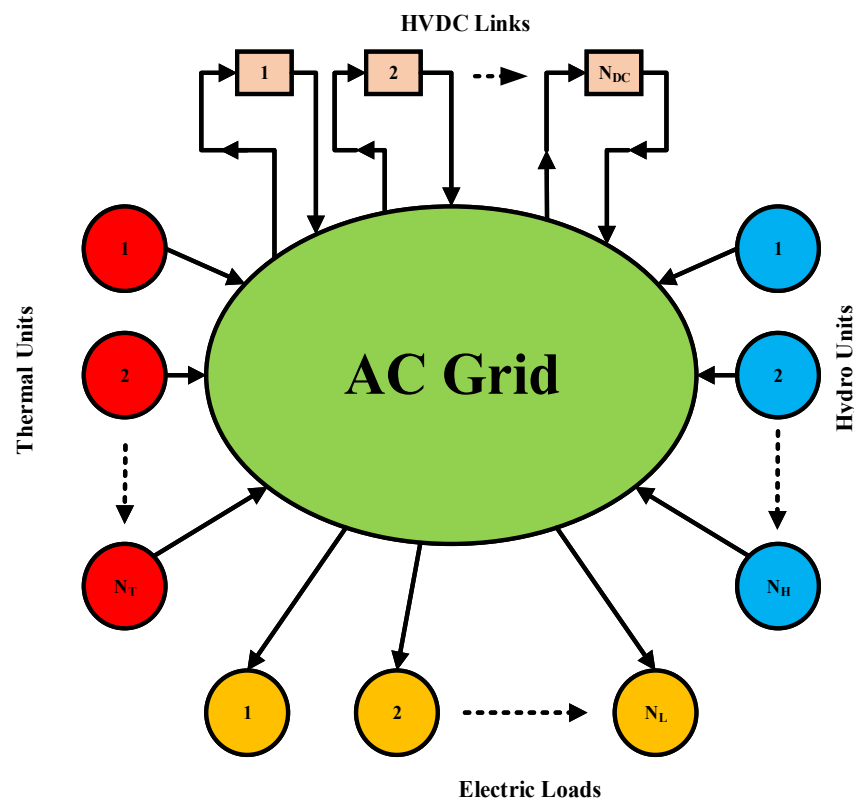


Figure 1. Generalized network diagram.

Figure 1 shows an electric network in which a number of hydel and thermal power plants are embedded. The inward arrows show that the power is delivered to the network. The loads are attached to the network. Here, outward arrows show the flow of power from the network to the loads. The HVDC blocks take power from certain buses (represented by outward arrows) and deliver it to other buses of the network (represented by inward arrows). The idea is to propose a Lagrange function for such a network considering all the generation, load, and network constraints. The following steps are being followed.

2.1. Hydrothermal Problem Formulation

The objective of hydrothermal is to utilize a given volume of water such that to minimize the production cost of N_T generating units subject to constraints of transmission lines, generators, and HVDC line limits. Therefore, the problem is formulated in general as $minimize \sum_{j=1}^{Jmax} \sum_{t=1}^{N_T} [F_t(P_{tj})]$ subject to constraints $p(x) = 0$ and $q(x) \leq 0$, where $p(x)$ and $q(x)$ are equality and inequality constraints, respectively. Equation $p(x)$ represents the network DC optimal power flow (DCOPF)-based load power balances, while Equation $q(x)$ denotes water volume discharge and minimum and maximum limits of hydro and thermal power generators. The cost of thermal generating units is approximated as a quadratic cost rate given in (1). Similarly, the water flow from hydro power plants in j time intervals is approximated using (2). The expressions (1) and (2) are used for the incremental cost of thermal power and fictitious cost of water, respectively, that must be paid to satisfy power balance, water volume, HVDC line limit, and generation constraints.

$$\sum_{j=1}^{Jmax} \sum_{t=1}^{N_T} [F_t(P_{tj})] = \sum_{j=1}^{Jmax} \sum_{t=1}^{N_T} [a_t(P_{tj})^2 + b_t P_{tj} + c_t] \tag{1}$$

$$\sum_{j=1}^{Jmax} n_j \sum_{h=1}^{N_H} q_h(P_{hj}) = \sum_{j=1}^{Jmax} n_j \sum_{h=1}^{N_H} [x_h(P_{hj})^2 + y_h P_{hj} + z_h] = q_{TOT} \tag{2}$$

2.2. HVDC Line Flow Problem Formulation

A point-to-point connected HVDC system consists of two converter stations, namely rectifier and inverter stations, as shown in Figure 2. Both converter stations are connected to AC systems on ‘r’ and ‘i’ nodes through filters and tap-changing transformers. Inverter station maintains DC bus voltage within limits and rectifier station controls the active power flow at specified value P_{flow} [24]. The power transfer in the system can be in either direction. In the previous research, the investigations have been carried out to optimize the controller gains to control the active power transfer in HVDC system [26]. HVDC problem formulation consists of the following steps.

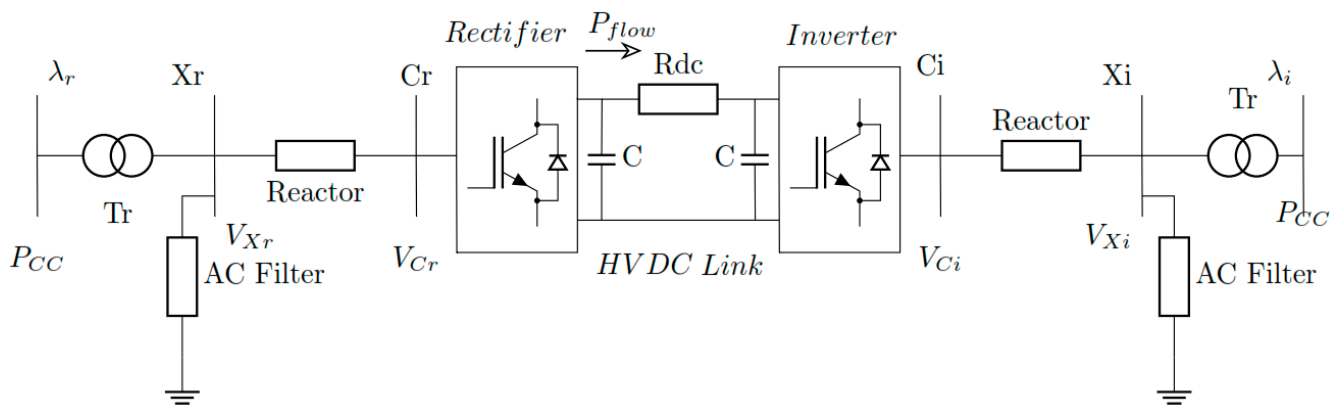


Figure 2. HVDC system.

Modelling of the point-to-point HVDC grids has been extensively performed to couple the VSC station with an AC network as an ideal voltage source either through an impedance or by phase shifting transformer for power flow analysis [27–31]. Similarly, intensive literature exists in the domain of economic dispatch for renewables ([32–36] and references therein). It is vital for economic dispatch applications to formulate the power flow equations

of HVDC link from inverter to rectifier and vice versa. The DC power flow expression from inverter and rectifier, respectively, are given in (3).

$$P_{dc_i} = (V_i^2 - V_i V_r) G_{dc}, P_{dc_r} = (V_r^2 - V_i V_r) G_{dc} \tag{3}$$

where V_i and V_r are inverter and rectifier voltages, respectively, and $G_{dc} = \frac{1}{R_{dc}}$.

To formulate the combined equations for HVDC power flow and AC grids, some basic assumptions are made on AC grid: (a) neglect conduction losses, i.e., $G_i = G_r = 0$, (b) set $V_i = V_r = 1$ p.u, and (c) due to very small angular difference, set $\sin(\theta_r - \theta_i) \cong (\theta_r - \theta_i)$. Hence, (6) takes the form for nodal power balances in various nodes of HVDC grid and defines the equality constraints for HVDC link. The resultant expression becomes as given in (4):

$$P_{ri} = (B_r - B_i)(\theta_r - \theta_i) \tag{4}$$

where B_r, B_i and θ_r, θ_i represent susceptance and phase angle on rectifier and inverter side, respectively. Susceptance is the inverse of reactance offered by AC filter, reactors, and transformer on either side of the converter.

2.3. AC Network Problem Formulation

The nodal power balance is formulated based on the operating point of the AC system. The power balance relation in (5) exhibits equality constraints $p(x)$ as a function of nodal power generation, demand, and calculated power in (6).

$$\Delta P_k = P_{gk} - P_{dk} - P_k^{cal} = 0 \tag{5}$$

$$P_K^{cal} = G_{kk} V_k^2 + \sum_{mek} V_k V_m [G_{km} \cos(\theta_k - \theta_m) + B_{km} \sin(\theta_k - \theta_m)] \tag{6}$$

where V_k, V_m and θ_k, θ_m are the voltage magnitudes and phase angles of the transmission lines linking buses 'k' and 'm', respectively. Moreover, G and B are conductance and susceptance of lines connecting the respective busses, respectively.

Under steady state condition of AC grid, $V_k = V_m = 1$ p.u and with negligible power loss $G_{kk} = G_{km} = 0$, the expression (6) reduces to $P_K^{cal} = \sum_{mek} B_{km}(\theta_k - \theta_m)$. Then, this expression can be generalized for lossless AC grids having α nodes in (7).

$$\begin{bmatrix} P_1 \\ \vdots \\ P_\alpha \end{bmatrix} = \begin{bmatrix} B_{11} & \dots & B_{1\alpha} \\ \vdots & \ddots & \vdots \\ B_{\alpha 1} & \dots & B_{\alpha\alpha} \end{bmatrix} \begin{bmatrix} \theta_1 \\ \vdots \\ \theta_\alpha \end{bmatrix} \implies [P] = [B][\theta] \tag{7}$$

where P is nodal power, B is susceptance, and θ is the nodal phase angle.

The mostly used HVDC links occur either in embedded or decoupled form with the AC grids [24]. These models are used for the investigation of optimal power flow in HVDC links connected to AC systems. The embedded HVDC link model deduces that both sending and receiving end converter stations consider same phase angles to AC grid. The expressions (4) and (7) provide the relationship between two AC grids connected HVDC link for sending and receiving end power flow. The mathematical expressions (1), (2), (4), and (7) are added in the Lagrange function to augment DCOPF-based AC grid details and HVDC flow limit in hydrothermal scheduling. The resultant expression is given in (8).

2.4. Overall Problem Formulation

The objective of the research is to minimize the thermal generation cost subject to meet the load balance, generator limit, HVDC line flow, and water consumption constraints. Based on the objective and constraints, the Lagrange function is stated as given in (8);

$$\mathcal{L} = \sum_{j=1}^{J_{max}} \left[\left(n_j \sum_{t=1}^{N_b} F_t(P_{tj}) \right) + \lambda_j^{N_b} \left([B_x][\theta]_j - (P_{thj} - P_{dj}) \right) + \lambda_j^{N_b+1} \left((P_{ri})_j - P_{HVDCset} \right) + \gamma \left(n_j \sum_{h=1}^{N_H} q_h(P_{hj}) - q_{TOT} \right) + \mu \left[g \left(P_{tj}^{min}, P_{tj}^{max}, P_{hj}^{min}, P_{hj}^{max} \right) \right] \right] \quad (8)$$

where n_j is the scheduling interval in hours, N_b is the number of buses, F_t is the thermal cost function which needs to be minimized subjected to power balance constraint $\left([B_x][\theta]_j - (P_{thj} - P_{dj}) \right)$ and water storage constraint $\left(n_j q_h(P_{hj}) = q_{TOT} \right)$, $\lambda_j^{N_b}$ is Lagrange multiplier which shows nodal marginal price of bus number N_b in j^{th} time interval in $\frac{\$}{MWh}$, P_{dj} is the load in each time interval, P_{thj} is the sum of power generated by thermal and hydro units in each time interval, $(P_{ri})_j$ is the actual power flow on HVDC link from rectifier to inverter, $P_{HVDCset}$ is the line flow limit of the HVDC link, P_{tj}^{min} and P_{tj}^{max} are minimum and maximum limits of thermal generators, P_{hj}^{min} and P_{hj}^{max} are minimum and maximum limits of hydro generators, γ is Lagrange multiplier which shows fictitious cost of water, H is number of hydro units, and q_{TOT} is the total water volume available for hydro power generation.

2.5. Constraints

The constraints of hydro and thermal power plants along with load balance and transmission limits are explained.

- Load balance constraints

$$P_{thj} = P_{dj} + [B_x][\theta]_j \quad (9)$$

where P_{thj} , P_{dj} , and $[B_x][\theta]_j$ are the total thermal and hydropower, load demands, and transmission line flows in j^{th} time intervals, respectively.

- Thermal plant generation limit

$$P_{tj}^{min} \leq P_{tj} \leq P_{tj}^{max} \quad (j = 1, 2, \dots, 24 \text{ h}) \quad (10)$$

where P_{tj}^{min} and P_{tj}^{max} are the minimum and maximum output of the N_T thermal power plants in j^{th} time intervals, respectively.

- Hydro plant generation limit

$$P_{hj}^{min} \leq P_{hj} \leq P_{hj}^{max} \quad (j = 1, 2, \dots, 24 \text{ h}) \quad (11)$$

where P_{Hj}^{min} and P_{Hj}^{max} are the minimum and maximum output of the N_H hydro power plants in j^{th} time intervals, respectively.

- Water volume limit

$$n_j \sum_{h=1}^{N_H} q_h(P_{hj}) = q_{TOT} \quad (j = 1, 2, \dots, 24 \text{ h}) \quad (12)$$

where q_{TOT} is the total water volume available for power generation and $q_h(P_{hj})$ is the water flow rate at the output power of P_{hj} hydro unit in n_j number of hours. Constant head is assumed to consume total available water volume for power generation in the j^{th} time intervals.

- HVDC line limitation

$$P_{ri}^{min} \leq P_{ri} \leq P_{ri}^{max} \quad (j = 1, 2, \dots, 24 \text{ h}) \quad (13)$$

This means power flow of lines is calculated by DC load flow to check the capacity limitations of HVDC link. In real scheduling, HVDC line limitations are obeyed as specified electric quantity trade limitations lines between regional distributors of electricity.

The proposed approach is a novel alternative to address fundamental problems, as it is structured to augment DC power flow in hydrothermal scheduling. Moreover, it is general to harmonize the number of HVDC links.

As already discussed, the quadratic cost expression, given in (1) of thermal power plants, does not include the power system network details, transmission line parameters, transmission line congestion constraints, HVDC links, etc. [37,38]. The expressions (1) and (2) only consider equality constraints of load balance and water volume. While considering the network constraints without line limits in an economic dispatch, the gradient method is used to solve the Lagrange equation [9]. Moreover, the Lagrange function considering all network constraints, hydrothermal, HVDC links, the generator’s extreme limits, and line limitations can be optimized by linear programming (LP). Hence, linear programming (LP) technique is used to solve combined hydrothermal scheduling with DCOPF considering generators’ inequality and HVDC line limit constraints. As per LP, the quadratic cost expression of thermal power plants does not satisfy the requirements. Therefore, a piecewise linear approximation of the cost function given in (1) is performed. The segment wise slopes of piecewise linear approximation are developed using (14).

$$S_a = \frac{F_{a+1} - F_a}{P_{a+1} - P_a} \text{ for } a = 1, 2, 3, \dots, N_s \text{ (Number of slope segments)} \quad (14)$$

In (14), the number of slope segments (N_s) depends on the minimum and maximum limits of thermal power generators and step size defined by the user.

Previously, (7) gave important information about the nodal power injection considering the network admittances without real part and help in finding the angles. However, (7) does not provide the line power flows. Therefore, the proposed approach considers the line flows, network constraints, generation limits, etc., formally in (15).

$$\left. \begin{aligned} \text{Minimize } F(P_t) &= F(P_t^{min}) + \sum_{a=1}^{N_s} \sum_{t=1}^{N_T} S_{at} P_{at} \\ \text{Subject to } P &= B\theta \\ P_B &= (D \times E) \times \theta \\ -P_B^{max} &\leq P_B \leq P_B^{max} \\ q_{TOT} &= \sum_{h=1}^{N_H} q_h(P_h) \\ 0 \leq P_{gk} &\leq P_{gk}^{max}, \forall k \in \{generator_{buses}\} \end{aligned} \right\} \quad (15)$$

where N_s is the number of slope segments, N_T is the number of thermal generators, P is the nodal power injections at all nodes, θ is nodal angle, P_B is line flow for AC and HVDC system, D and E are node-arc matrices, and $-P_B^{max}$ and P_B^{max} are line flow limits. The q_{TOT} is the total water volume available for generation, N_H is the number of hydro units, and q_h is the water discharge rate to generate hydro power P_h in an interval. Moreover, (15) is similar to (8) with constraints mentioned as Lagrange multipliers.

3. Research Methodology

The proposed linear programming based on Lagrange multipliers research methodology shown in Figure 3 has been successfully implemented on a case study power system network shown in Figure 4 by carrying out the following steps.

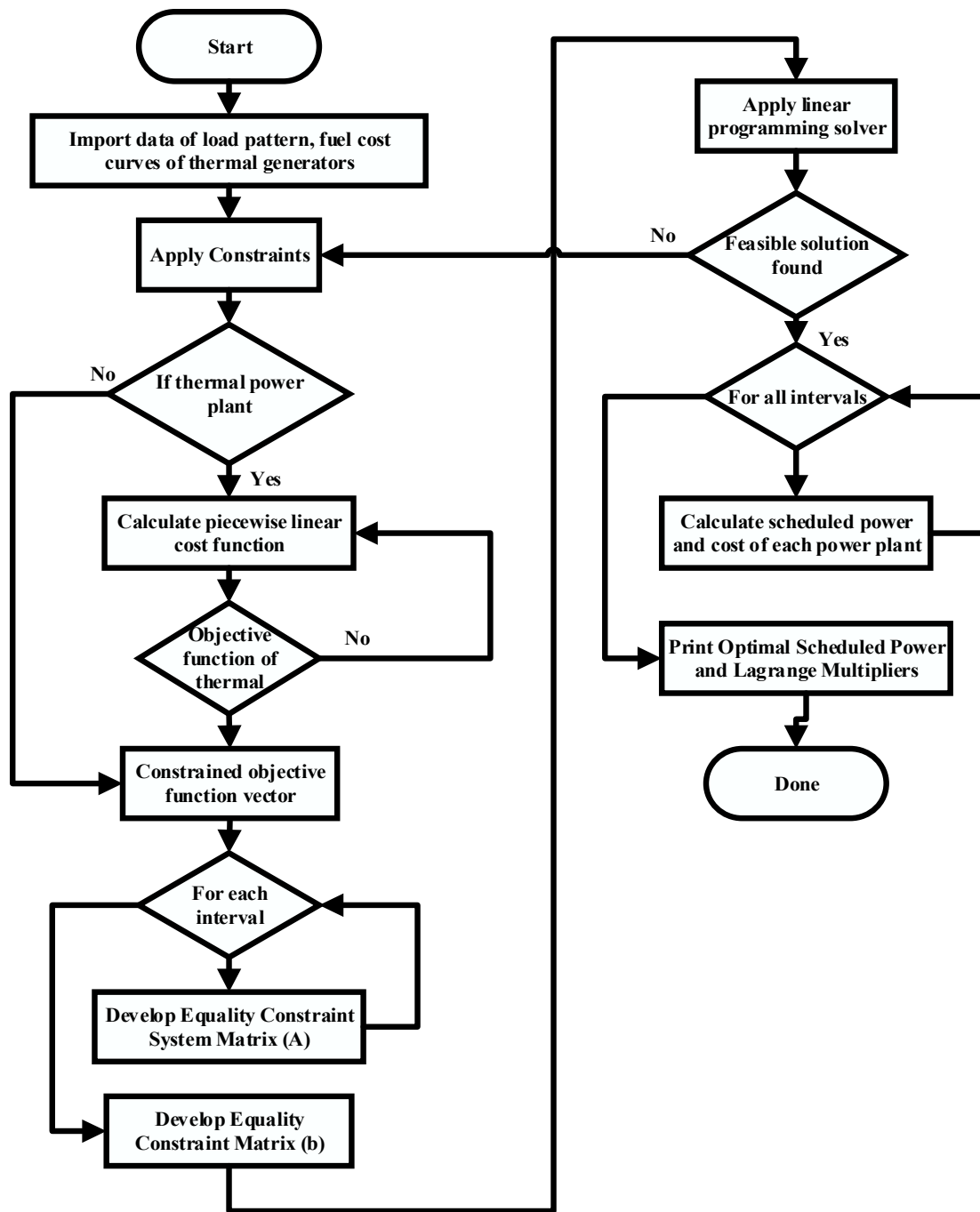


Figure 3. Algorithm flow chart.

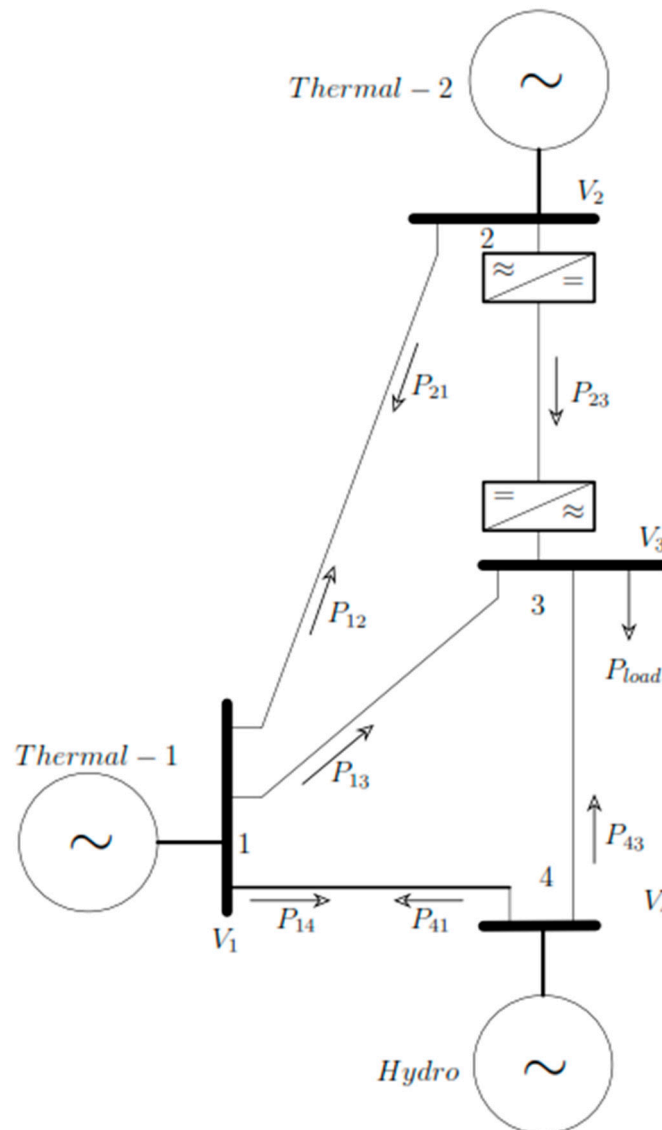


Figure 4. Four (4) bus AC system with HVDC link.

3.1. Objective Function

The objective function is given in (16);

$$f(x) = Ax = \begin{bmatrix} s_1 & s_2 & 0 & 0 & 0 & 0 & 0 & 0 & 0 & 0 & 0 & 0 & 0 & 0 \\ P_{t1} & P_{t2} & P_h & P_{B1} & P_{B2} & P_{B3} & P_{B4} & P_{B5} & \theta_1 & \theta_2 & \theta_3 & \theta_4 & W \end{bmatrix}^T \quad (16)$$

In (16), the dimensions of 's₁' and 's₂' (in the row) depend on the number of slopes based on step size, while P_t^{min} and P_t^{max} depend on the limits of the thermal power station.

3.2. Output Vector

The output vector 'x' for the given case study network and constraints is defined in (17).

$$x = \begin{bmatrix} P_t & P_h & P_B & \theta & W \end{bmatrix}^T = \begin{bmatrix} P_{t1} & P_{t2} & P_h & P_{B1} & P_{B2} & P_{B3} & P_{B4} & P_{B5} & \theta_1 & \theta_2 & \theta_3 & \theta_4 & W \end{bmatrix}^T \quad (17)$$

where P_t is the incremental generation vector for two thermal generators connected to bus-1 and bus-2, P_h is hydropower generation, P_B is the line power flows vector for five branches,

θ is the vector of angles for all four buses in radian, and W is the water volume variable. All these variables are added as equality constraints given in (15) to a single matrix relation. For single matrix relation, one kind of equality constraint is given as injected powers and another kind of equality constraint is given as line power flows as in (15), resulting in (18) and (19).

$$-P_B + (D \times E) \times \theta = 0 \tag{18}$$

$$-P + B\theta = 0 \tag{19}$$

3.3. Equality Constraints

The equality constraints are given in (18) and (19). Matrix ($Ax = b$) form of equality constraints requires dimensions. The dimensions of equality constraints based on the case study are:

- Number of columns: As the vector x has 13×1 , matrix A should have 13 columns to multiply x .
- Number of rows: As there are five branches, four buses, and one water volume constraint, (18) and (19) will have to contribute a total of ten (10) rows to matrix A .

Therefore, the dimension of matrix A will be 10×13 . Let us start from line power flow as in (18). The D -matrix is given in (20). The node-arc matrix E , is given as (21):

$$D = \begin{bmatrix} B_1 & 0 & 0 & 0 & 0 \\ 0 & B_2 & 0 & 0 & 0 \\ 0 & 0 & B_3 & 0 & 0 \\ 0 & 0 & 0 & B_4 & 0 \\ 0 & 0 & 0 & 0 & B_5 \end{bmatrix} \tag{20}$$

$$E = \begin{bmatrix} 1 & 0 & 0 & -1 \\ 1 & -1 & 0 & 0 \\ 0 & 1 & -1 & 0 \\ 0 & 0 & -1 & 1 \\ 1 & 0 & -1 & 0 \end{bmatrix} \tag{21}$$

The product $D \times E$ required to find line power flows is given as (22):

$$D \times E = \begin{bmatrix} B_1 & 0 & 0 & 0 & 0 \\ 0 & B_2 & 0 & 0 & 0 \\ 0 & 0 & B_3 & 0 & 0 \\ 0 & 0 & 0 & B_4 & 0 \\ 0 & 0 & 0 & 0 & B_5 \end{bmatrix} \begin{bmatrix} 1 & 0 & 0 & -1 \\ 1 & -1 & 0 & 0 \\ 0 & 1 & -1 & 0 \\ 0 & 0 & -1 & 1 \\ 1 & 0 & -1 & 0 \end{bmatrix} = \begin{bmatrix} B_1 & 0 & 0 & -B_1 \\ B_2 & -B_2 & 0 & 0 \\ 0 & B_3 & -B_3 & 0 \\ 0 & 0 & -B_4 & B_4 \\ B_5 & 0 & -B_5 & 0 \end{bmatrix} \tag{22}$$

The elements of (22) will be placed in the upper right corner of matrix A from columns 9 to 12. The first eight columns of the top five rows will be multiplied to generated powers (P_{t1}, P_{t2}, P_t) and line power flows ($P_{B1}, P_{B2}, P_{B3}, P_{B4}, P_{B5}$) variables. As generation variables are not used within the line power flow equations, the first three (3) columns of the top five rows will be zeros. The columns (4–8) will be zeros, except a single element in each row will be -1 to obtain corresponding line power flows.

DC power flow equations corresponding to (19) are written in matrix A . The augmented DC power flow matrix is given as (23):

$$B = \begin{bmatrix} B_{11} & -B_{12} & -B_{13} & -B_{14} \\ -B_{21} & B_{22} & -B_{23} & -B_{24} \\ -B_{31} & -B_{32} & B_{33} & -B_{34} \\ -B_{41} & -B_{42} & -B_{43} & B_{44} \end{bmatrix} \tag{23}$$

Elements of (23) will be placed at the lower right of matrix A from rows 6 to 9 and columns 9 to 12. The first three (3) columns of matrix A are reserved for generation variables. The expression (19) requires negative injections for all buses and injected power is $P_{th} - P_d$. However, load variables are not added in matrix A, which will be placed on the right side of the expression $Ax = b$ in matrix b. Additionally, generated power from generation plants will be placed with a negative sign in the rows starting from 6 to 9 and the first three (3) columns with respect to the respective bus in matrix A. Hydro power plant and water volume constraints are added to the last (10th) row and column 3rd and 13th of the matrix A, respectively. The resultant expression $Ax = b$ in matrix form is given in (24):

$$Ax = b \Rightarrow \begin{bmatrix} 0 & 0 & 0 & -1 & 0 & 0 & 0 & 0 & B_1 & 0 & 0 & -B_1 & 0 \\ 0 & 0 & 0 & 0 & -1 & 0 & 0 & 0 & B_2 & -B_2 & 0 & 0 & 0 \\ 0 & 0 & 0 & 0 & 0 & -1 & 0 & 0 & 0 & B_3 & -B_3 & 0 & 0 \\ 0 & 0 & 0 & 0 & 0 & 0 & -1 & 0 & 0 & 0 & -B_4 & B_4 & 0 \\ 0 & 0 & 0 & 0 & 0 & 0 & 0 & -1 & B_5 & 0 & -B_5 & 0 & 0 \\ -1 & 0 & 0 & 0 & 0 & 0 & 0 & 0 & B_{11} & -B_{12} & -B_{13} & -B_{14} & 0 \\ 0 & -1 & 0 & 0 & 0 & 0 & 0 & 0 & -B_{21} & B_{22} & -B_{23} & -B_{24} & 0 \\ 0 & 0 & 0 & 0 & 0 & 0 & 0 & 0 & -B_{31} & -B_{32} & -B_{33} & -B_{34} & 0 \\ 0 & 0 & -1 & 0 & 0 & 0 & 0 & 0 & -B_{41} & -B_{42} & -B_{43} & B_{44} & 0 \\ 0 & 0 & q(2) * n & 0 & 0 & 0 & 0 & 0 & 0 & 0 & 0 & 0 & 1 \end{bmatrix} \begin{bmatrix} P_{t1} \\ P_{t2} \\ P_h \\ P_{B1} \\ P_{B2} \\ P_{B3} \\ P_{B4} \\ P_{B5} \\ \theta_1 \\ \theta_2 \\ \theta_3 \\ \theta_4 \\ W \end{bmatrix} = \begin{bmatrix} 0 \\ 0 \\ 0 \\ 0 \\ 0 \\ P_{t1}^{min} \\ P_{t2}^{min} \\ -P_{load} \\ P_h^{min} \\ W_{start} + inflow - q(1) * n \end{bmatrix} \tag{24}$$

3.4. Inequality Constraints

These constraints are simple and are given in (25):

$$\begin{bmatrix} 0 \\ 0 \\ 0 \\ -P_{B1}^{max} \\ -P_{B2}^{max} \\ -P_{B3}^{max} \\ -P_{B4}^{max} \\ -P_{B5}^{max} \\ -\pi \\ -\pi \\ -\pi \\ -\pi \\ W_{end} \end{bmatrix} \leq \begin{bmatrix} P_{t1} \\ P_{t2} \\ P_h \\ P_{B1} \\ P_{B2} \\ P_{B3} \\ P_{B4} \\ P_{B5} \\ \theta_1 \\ \theta_2 \\ \theta_3 \\ \theta_4 \\ W \end{bmatrix} \leq \begin{bmatrix} step \\ step \\ P_h^{max} \\ P_{B1}^{max} \\ P_{B2}^{max} \\ P_{B3}^{max} \\ P_{B4}^{max} \\ P_{B5}^{max} \\ \pi \\ \pi \\ \pi \\ \pi \\ W_{start} + \max(w) \end{bmatrix} \tag{25}$$

In (25), the dimensions of P_{t1} and P_{t2} depend on the number of slope segments based on P_{t1}^{min} and P_{t1}^{max} values of the thermal power generating stations. Hence, the row-wise size of columns 1 and 2 will depend on the number of slope segments. The expressions (24) and (25) are applicable to single load interval. For 24 h or daily load intervals, these equations are modified as in (26):

$$Ax = b \Rightarrow \begin{bmatrix} A_{11} & 0 & 0 & \dots & \dots & 0 \\ C_{11} & A_{22} & 0 & \dots & \dots & 0 \\ 0 & C_{22} & A_{33} & \dots & \dots & 0 \\ \vdots & \vdots & \vdots & \ddots & \ddots & \vdots \\ 0 & 0 & 0 & \dots & A_{(i-1)(j-1)} & 0 \\ 0 & 0 & 0 & \dots & C_{(i-1)(j-1)} & A_{ij} \end{bmatrix} \begin{bmatrix} x_{11} \\ x_{21} \\ x_{31} \\ \vdots \\ \dots \\ x_{i1} \end{bmatrix} = \begin{bmatrix} b_{11} \\ b_{21} \\ b_{31} \\ \vdots \\ \dots \\ b_{i1} \end{bmatrix} \tag{26}$$

where A_{ij} and $C_{(i-1)(j-1)}$ matrices have dimensions 10×13 , having ten rows and thirteen columns for each load interval; $i = j$ is the number of load intervals (1, 24 h). The elements of matrix A are shown in (24) for a single load interval. The elements of matrix C are given as in (27):

$$C = \begin{bmatrix} \text{Zeros}(9 \times 12) & \text{Zeros}(9 \times 1) \\ \text{Zeros}(1 \times 12) & -1 \end{bmatrix} \tag{27}$$

Equation (27) is only used as leftover water volume in one interval to be used in the next load interval in constraint expression (24). Inequality constraints for a single load period given in (25) are modified for 24 h load intervals accordingly. The algorithm flow chart of the proposed approach is shown in Figure 3 to implement (8) using (15) with constraints from (9) to (13) and realistic equations from (16) to (27) for all load periods in MATLAB Software.

The detailed step-by-step implementation procedure of the proposed approach in MATLAB Software is given in Table 1.

Table 1. Step-by-step implementation of proposed procedure.

Step-by-Step Implementation of Proposed Procedure for Coordinated/Optimal Economic Operation of Hydrothermal Units with HVDC Link Based on Lagrange Multipliers	
1	Consider a power system network having ' N_b ' number of buses and ' N_M ' number of branches (shown in Figure 4).
2	Calculate the susceptance of each line following nodal power injection using (5), (6), and (7) of AC network and (4) for HVDC network or directly follow (10) which is common for both hydrothermal-based AC and HVDC power system.
3	Find slopes of cost functions of all thermal generators using (14) and define an objective function based on (16).
4	Formulate the DCOPF coordinated economic dispatch problem using (8) and (15)
5	Find a single matrix for all equality constraints, load balance, line power flows, and nodal power injections using (9), (18), and (19), respectively. This can be executed using node-arc incidence matrix product ($D \times E$) using (22).
6	Embed hydropower plant variable and water volume constraint using (11) and (12). Then, develop a standard form of the matrix ($Ax = b$) using (24) for linear programming (LP).
7	Find parameters for b-matrix (of $Ax = b$) using load and generation buses of power system network (shown in Figure 4) and objection function given in (15).
8	Define inequality constraints of the power system network under study using (10), (11), and (13).
9	Apply the standard linear programming (LP) method using MATLAB software.
10	Check constraints. If all constraints are satisfied, then procedure is done. Otherwise, go to step 3.
11	Print the optimal operating schedule and nodal price of each bus.

4. Results and Discussion

A case study is designed to verify the effectiveness of the proposed methodology. Four bus AC systems with two AC grids are interconnected by point-to-point HVDC transmission link, shown in Figure 4. It is ensured that the modelled HVDC link agrees with (4). The cost curves of the thermal power plant and flow rate characteristics of the hydro power plant are shown in Tables 2 and 3, respectively.

Table 2. Thermal plants characteristics.

Unit	$a_t \left[\frac{\$}{\text{MW}^2\text{h}} \right]$	$b_t \left[\frac{\$}{\text{MWh}} \right]$	$c_t \left[\frac{\$}{\text{h}} \right]$	$P_t^{\min} (\text{MW})$	$P_t^{\max} (\text{MW})$
Thermal-1	0.0033	10.8	1200	25	875
Thermal-2	0.003	12.6	1710	40	600

Table 3. Hydro plant characteristics.

Unit	$x_h \left[\frac{\text{AF}}{\text{MW}^2\text{h}} \right]$	$y_h \left[\frac{\text{AF}}{\text{MWh}} \right]$	$z_h \left[\frac{\text{AF}}{\text{h}} \right]$	$P_h^{\min} (\text{MW})$	$P_h^{\max} (\text{MW})$	$q_{\text{TOT}} (\text{AF})$
Hydro	0	4.9	50	0	500	30,000

The power system network has five transmission lines connected to four different buses. The transmission line connected between bus-2 and bus-3 is considered an HVDC link. This line has point-to-point converter stations connected to the respective buses. It is assumed that all the AC lines have equal admittance with the assumption of zero real parts. Thermal unit-1 connected to bus-1 can generate a minimum power of 25 MW and a maximum power of 875 MW. However, thermal unit-2 connected to bus-2 can produce a minimum of 40 MW and a maximum of 600 MW. The hydro plant connected to bus-4 can produce a maximum of 500 MW output. The initial volume of water is 15,000 Acre-feet (AF). The allowed inflow is 1250 AF per hour. For the 24 h period, the total water available for power generation is 30,000 AF. The required ending capacity of the reservoir is 15,000 AF.

Two scenarios are implemented in Figure 4 network: (i) DCOPF including hydrothermal scheduling without line trading limitation on the HVDC line and (ii) DCOPF including hydrothermal scheduling with line trading limitation ($P_{\text{HVDC}} = 400 \text{ MW}$) on the HVDC line. Only HVDC line has direction power flow constrain, whereas all the other lines have flexibility in the flow of power on either side.

The load is connected to bus-3 and the daily load on the four-bus system is shown in Figure 5.

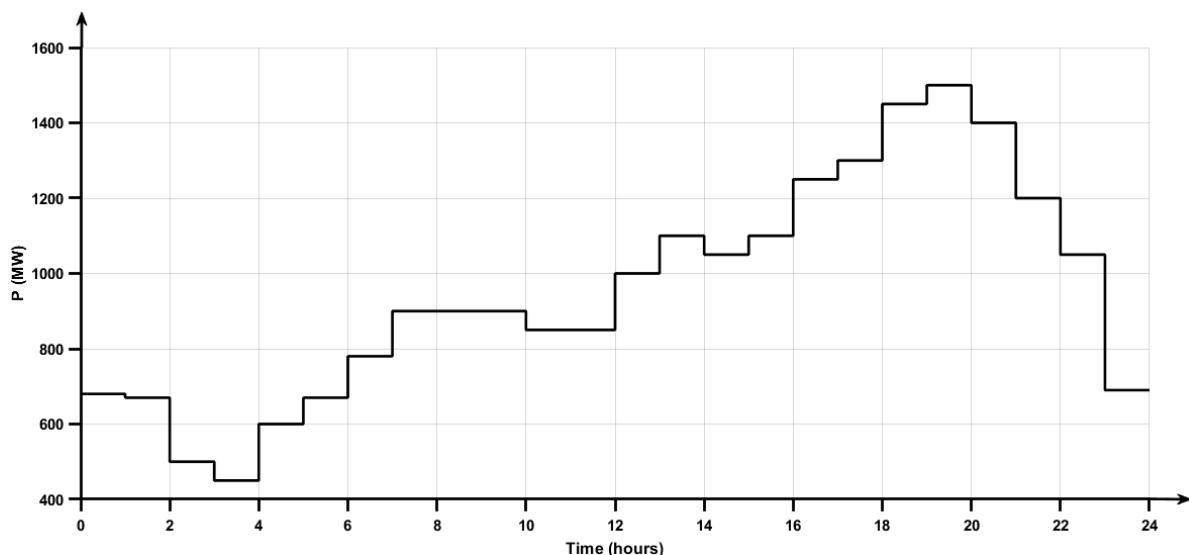


Figure 5. Load pattern on network.

Figure 6 shows the power contribution (bar charts) of each generating station to meet the load demand. The power shared by the hydro unit to load is based on the availability of water for power generation. The power shared by both thermal units to load demand is optimized based on their cost rate characteristics shown in Table 2. Therefore, the cost of thermal power units is the minimum for typical load demand in a specific time period.

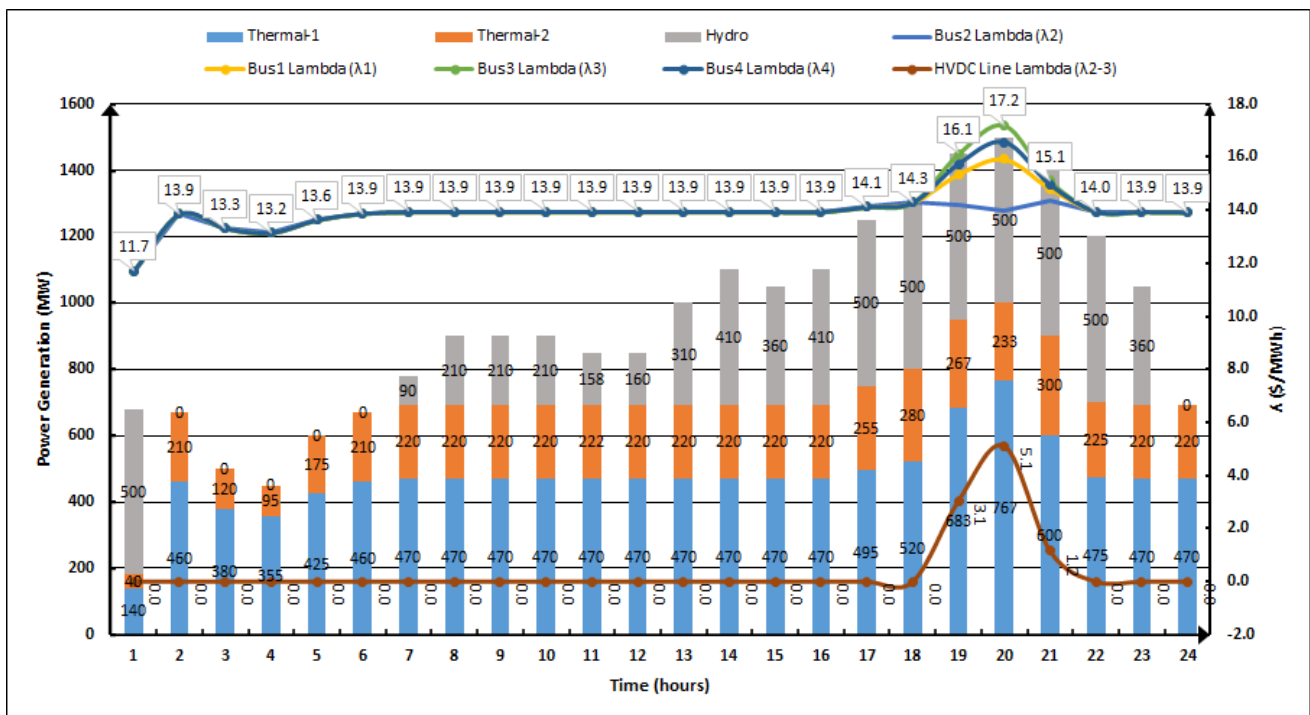


Figure 6. Hydrothermal scheduled power, bus price, and line limit price.

Due to combined investigations of economic hydrothermal scheduling and DCOPT at the same time, the system lambdas (λ) represent the bus location marginal price (LMP) or nodal price and line congestion price instead of the generator’s incremental cost. Figure 6 shows both lambdas (λ) under two different scenarios.

4.1. Scenario-1: Infinite HVDC Line Capacity

When the power system network shown in Figure 4 is operating under normal conditions, there is no capacity limit on the HVDC transmission line. Then, the lambda (λ) of each bus is constant for a specific load period, as shown in Figure 6. In this figure, for the first load interval, the load demand is 680 MW, and the nodal price is fixed (11.7 \$/MWh) for each bus. In the first interval, the hydro plant contribution is maximum. During the second load interval, load demand is 670 MW, and the nodal price is fixed (13.9 \$/MWh) for each bus with zero power contribution by the hydro plant. Similarly, for load periods 1 to 18th and 22nd to 24th, nodal prices of all buses are fixed when there is an infinite line capacity limit. The resultant HVDC line limit lambda (λ_{2-3}) is zero for these load intervals due to the infinite line capacity limit; the network considered it as a single bus. The respective power flow in each line branch and each interval is shown in Figure 7. The optimal power generation of each generating station to meet the load demand in each interval is shown in Figure 8.

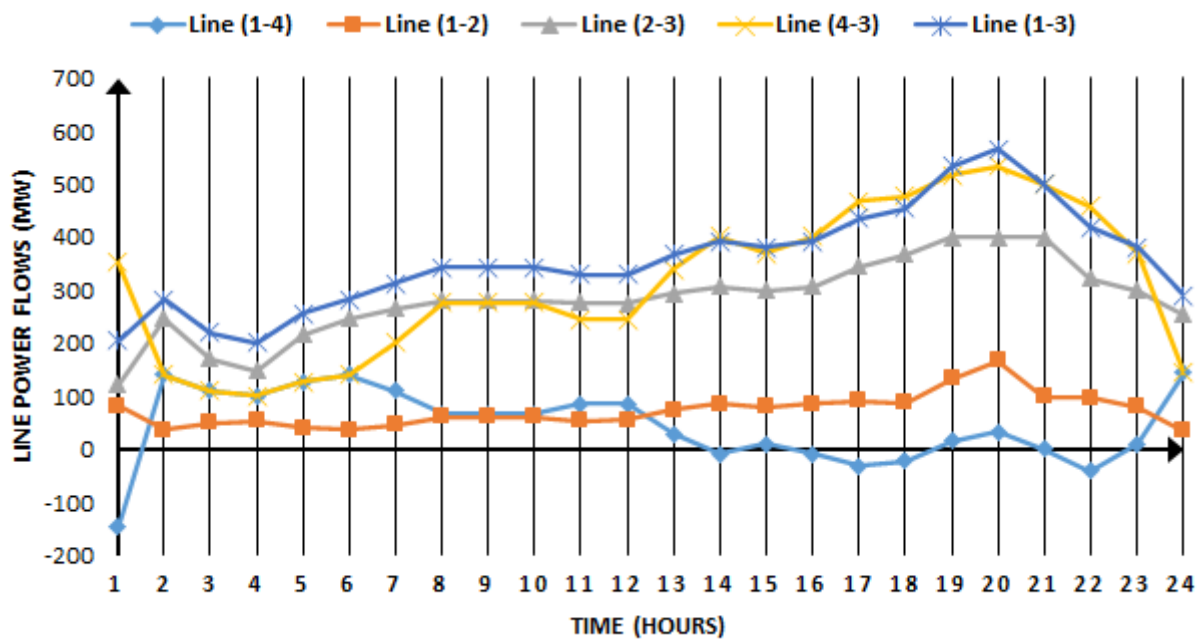


Figure 7. Line power flow during each load interval.

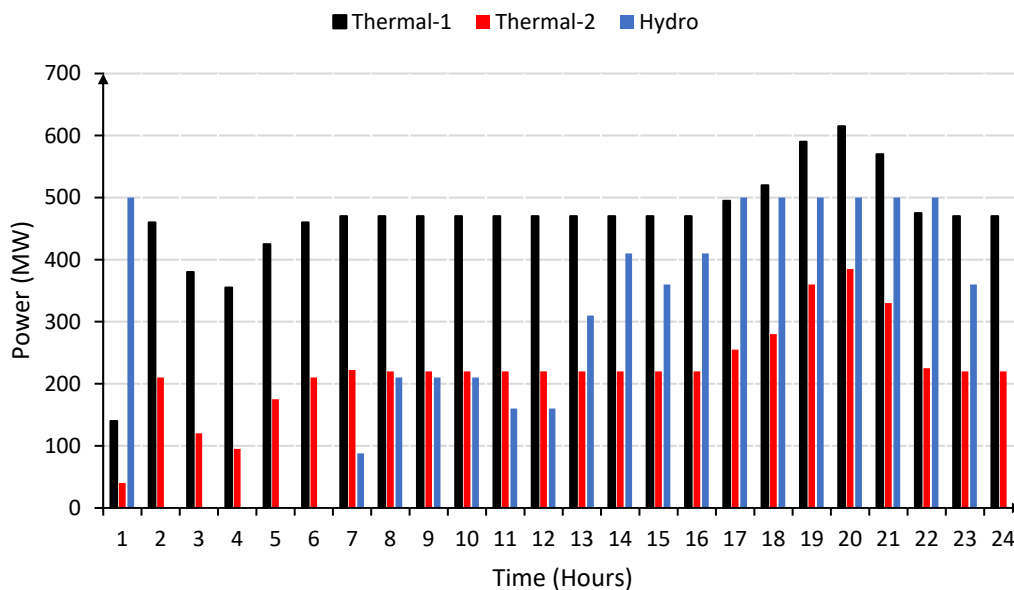


Figure 8. Generators optimal power during each load interval in infinite line capacity.

4.2. Scenario-2: Limited HVDC Line Capacity

In this case, line trading limitation $P_{Line2-3} = P_{HVDC} = 400$ MW is added on the HVDC link shown in Figure 4. The load power demand during time intervals 19, 20, and 21 is 1450 MW, 1500 MW, and 1400 MW, respectively, as shown in Figure 5. During these time intervals, the power shared by a hydro unit is 500 MW, thermal-1 is 683 MW, 767 MW, and 600 MW, and thermal-2 is 267 MW, 233 MW, and 300 MW, as given in Figure 6. Due to HVDC line limitations, the power is diverted to other transmission lines of the network. Hence, the network does not consider a single bus which results in different buses' nodal lambdas (λ) price and line (λ) price. This makes the nodal price at bus-1 = $\lambda_1 = 15.4$ \$/MWh, bus-2 = $\lambda_2 = 14.2$ \$/MWh, bus-3 = $\lambda_3 = 16.1$ \$/MWh, and bus-4 = $\lambda_4 = 15.7$ \$/MWh, as shown in Figure 7. The line limit price in three different time intervals increased from 0 \$/MWh to 3.1 \$/MWh and 5.1 \$/MWh due to line congestion heating and losses. The line limit price is shown in Figure 7. Moreover, the optimal power generation of each

generating station to meet the load demand in each interval with limited line capacity is shown in Figure 9.

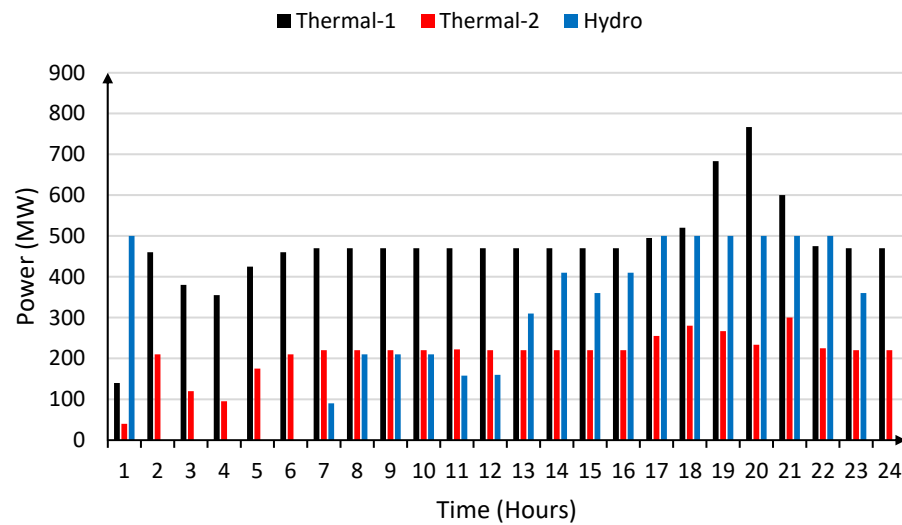


Figure 9. Generators optimal power during each load interval in limited line capacity.

The results described in both scenarios depict that all the buses’ nodal prices are the same for specific time interval loads when there are no line limitations. Additionally, the line price is zero. Meanwhile, when there are line capacity limitations, the bus nodal price increases from 14.3 \$/MWh to 17.2 \$/MWh and the line price increases from 0 \$/MWh to 5.1 \$/MWh. This results in total cost of power generation by the thermal-1 unit in 24 h period being \$170,921.4 and the thermal-2 unit being \$108,104 with $P_{HVDC} = 400$ MW limit. However, thermal-1 unit in 24 h period costs \$166,739.8 and the thermal-2 unit costs \$112,082.5 without HVDC line limitation. The proposed approach optimally scheduled the outputs of thermal generating stations under both scenarios to minimize the operating cost. It can be concluded that limited capacity HVDC links may change the optimal operating points of all generating stations throughout the load intervals. Hence, the electricity market will affect generation companies (GENCOs) and transmission system operators (TSO). Therefore, the proposed approach will be helpful in complex hydrothermal scheduling including embedded HVDC lines in existing AC networks for GENCOs and TSO to find their power generation price, bus nodal price, and line limit price.

The effectiveness of the proposed approach has been compared using interior-point and dual-simplex method. The results are presented in Table 4.

Table 4. Comparison of different techniques.

Parameters	Proposed Method	Interior-Point Method	Dual-Simplex Method
No. of iterations	6	10	292
Computational time (sec)	1.05	1.58	2.93

The interior-point method solves formulated problems in 10 iterations while dual-simplex uses 292 iterations without changing any other results. However, the proposed method takes only six iterations to solve the problem.

5. Conclusions

This research article has investigated the optimal operating point of hydrothermal power plants on AC networks with the limited capacity of an HVDC line under the different operating constraints. Modelling of AC power system including VSC-HVDC link has been

described for hydrothermal scheduling. The method is computationally efficient as it considers linear model of AC network with HVDC transmission link including DCOF. Nodal bus power injection matrix is modified to embed line flow constraint in DCOF. The quadratic cost curves of thermal generators are linearized segment wise to include the minimum and maximum generation limits. The hydro power plant is operated at maximum power ($P_h = 500$ MW) to obtain maximum efficiency. HVDC transmission line flow was successfully limited at $P_{HVDC} = 400$ MW. The Lagrange multipliers method is used for optimal operation of hydrothermal plants on power networks. The proposed formulation is applied to two scenarios of a case study. In the first scenario of the case study, the total thermal generation cost comes out to \$278,822.3. In the second scenario of the case study, the total cost of thermal generation is \$279,025.4. The difference in cost in both scenarios is minimum. It is observed in both scenarios, with the change in load, that this algorithm optimally selects the thermal generator to redispatch to meet the load demand and other line constraints with minimum cost.

The proposed approach can be extended to perform hydrothermal scheduling on seasonal load changes and deregulated electricity market in the future.

Author Contributions: Conceptualization, A.A. (Ali Ahmed); data curation, S.A.R.K.; formal analysis, A.A. (Arslan Ashraf) and M.M.G.; funding acquisition, M.A. and M.K.; investigation, S.A.R.K.; methodology, M.M.G.; project administration, M.K.; resources, A.A. (Ali Ahmed), A.A. (Arslan Ashraf), M.A. and M.K.; software, A.A. (Ali Ahmed) and A.A. (Arslan Ashraf); supervision, M.A.; validation, A.A. (Arslan Ashraf) and M.M.G.; visualization, M.A.; writing—original draft, A.A. (Ali Ahmed); writing—review and editing, S.A.R.K. and M.K. All authors have read and agreed to the published version of the manuscript.

Funding: The authors would like to acknowledge the support received from Saudi Data and AI Authority (SDAIA) and King Fahd University of Petroleum and Minerals (KFUPM) under SDAIA-KFUPM Joint Research Center for Artificial Intelligence Grant No. JRC-AI-RFP-08, Dhahran 31261, KSA. Additionally, the authors would like to thank King Khalid University for its financial support to this study.

Data Availability Statement: Not applicable.

Conflicts of Interest: The authors declare no conflict of interest.

Nomenclature

P_{hj}	Output power (MW) of h^{th} hydro unit in j^{th} period
P_{tj}	Output power (MW) of t^{th} thermal unit in j^{th} period
$F_t(P_{tj})$	Fuel cost rate (\$/hour) for t^{th} unit in j^{th} period
$q_h(P_{hj})$	Water flow rate (Acre-feet/hour) for h^{th} unit in j^{th} period
N_T	Number of thermal power plants
N_H	Number of hydro power plants
N_b	Number of buses
N_M	Number of lines (branches)
$P_{thj} = P_{tj} + P_{hj}$	Total output power (MW) of t^{th} thermal and h^{th} hydro unit in j^{th} period
J_{max}	Maximum number of periods
n_j	Number of hours in j^{th} period
a_t, b_t, c_t	Cost coefficients of t^{th} thermal unit
x_h, y_h, z_h	Water flow rate coefficients of h^{th} hydro unit
q_{TOT}	Total water volume available for power generation
\mathcal{L}	Lagrange function
λ, γ, μ	Lagrange multipliers
P_{flow}	HVDC line power flow limit
R_{dc}	Resistance of HVDC line

λ_r	Locational marginal Price (LMP) of rectifier bus
λ_i	Locational marginal Price (LMP) of inverter bus
PCC	Point of common coupling (PCC)
Tr	Coupling transformer
V_{X_r}, V_{C_r}	Voltage at bus X_r and C_r on rectifier side
V_{X_i}, V_{C_i}	Voltage at bus X_i and C_i on inverter side
C	DC link capacitor
ΔP_k	k^{th} bus nodal power balance
P_{gk}	Power generation on k^{th} bus
P_{dk}	Power demand on k^{th} bus
P_k^{cal}	Calculated nodal power on k^{th} bus
G_{km}	Conductance of line connecting bus node k and m
B_{km}	Susceptance of line connecting bus node k and m
θ	Nodal phase angle
Subscript k, m	Indicate the nodal bus
Subscript i, r	Indicate the inverter and rectifier, respectively
V	Bus voltage magnitude
$p.u$	Per unit quantity
DCOPF	Direct current optimal power flow
HVDC	High voltage direct current
N_s	Number of segments of quadratic cost function
S_a	Slope of quadratic cost function
T	Transpose of matrix
W	Water volume
P_B	Line power flow

References

- Kazantsev, Y.V.; Glazyrin, G.V.; Khalyasmaa, A.I.; Shayk, S.M.; Kuparev, M.A. Advanced Algorithms in Automatic Generation Control of Hydroelectric Power Plants. *Mathematics* **2022**, *10*, 4809. [\[CrossRef\]](#)
- Sibtain, D.; Gulzar, M.M.; Murtaza, A.F.; Murawwat, S.; Iqbal, M.; Rasool, I.; Hayat, A.; Arif, A. Variable structure model predictive controller based gain scheduling for frequency regulation in renewable based power system. *Int. J. Numer. Model. Electron. Netw. Devices Fields* **2022**, *35*, e2989. [\[CrossRef\]](#)
- Tan, K.; Tian, Y.; Xu, F.; Li, C. Research on Multi-Objective Optimal Scheduling for Power Battery Reverse Supply Chain. *Mathematics* **2023**, *11*, 901. [\[CrossRef\]](#)
- Grisales-Noreña, L.F.; Cortés-Caicedo, B.; Alcalá, G.; Montoya, O.D. Applying the Crow Search Algorithm for the Optimal Integration of PV Generation Units in DC Networks. *Mathematics* **2023**, *11*, 387. [\[CrossRef\]](#)
- Gul, M.; Tai, N.; Huang, W.; Nadeem, M.H.; Ahmad, M.; Yu, M. Technical and Economic Assessment of VSC-HVDC Transmission Model: A Case Study of South-Western Region in Pakistan. *Electronics* **2019**, *8*, 1305. [\[CrossRef\]](#)
- Bento, P.; Pina, F.; Mariano, S.; Calado, M.D.R. Short-term Hydro-thermal Coordination By Lagrangian Relaxation: A New Algorithm for the Solution of the Dual Problem. *KnE Eng.* **2020**, 728–742. [\[CrossRef\]](#)
- Gulzar, M.M.; Murawwat, S.; Sibtain, D.; Shahid, K.; Javed, I.; Gui, Y. Modified Cascaded Controller Design Constructed on Fractional Operator ‘ β ’ to Mitigate Frequency Fluctuations for Sustainable Operation of Power Systems. *Energies* **2022**, *15*, 7814. [\[CrossRef\]](#)
- Saini, O.; Chauhan, A. Optimal Operation of Short-Term Variable-Head Hydrothermal Generation Scheduling Using the Differential Evolution Method, Newton-Raphson Method and Heuristic Search Method. In Proceedings of the 1st International Conference on Recent Innovation in Electrical, Electronics and Communication System, RIEECS, Bhubaneswar, India, 27–28 July 2018.
- Wood, A.J. *Power Generation, Operation, and Control*, 3rd ed.; John Wiley & Sons: Hoboken, NJ, USA, 2014.
- Jian, J.; Pan, S.; Yang, L. Solution for short-term hydrothermal scheduling with a logarithmic size mixed-integer linear programming formulation. *Energy* **2019**, *171*, 770–784. [\[CrossRef\]](#)
- Gjerden, K.S.; Helseth, A.; Mo, B.; Warland, G. Hydrothermal scheduling in Norway using stochastic dual dynamic programming; a large-scale case study. In Proceedings of the 2015 IEEE Eindhoven PowerTech, Eindhoven, The Netherlands, 29 June–2 July 2015; pp. 1–6. [\[CrossRef\]](#)
- Fakhar, M.S.; Liaquat, S.; Kashif, S.A.R.; Rasool, A.; Khizer, M.; Iqbal, M.A.; Baig, M.A.; Padmanaban, S. Conventional and Metaheuristic Optimization Algorithms for Solving Short Term Hydrothermal Scheduling Problem: A Review. *IEEE Access* **2021**, *9*, 25993–26025. [\[CrossRef\]](#)
- Iqbal, M.; Gulzar, M.M. Master-slave design for frequency regulation in hybrid power system under complex environment. *IET Renew. Power Gener.* **2022**, *16*, 3041–3057. [\[CrossRef\]](#)

14. Gulzar, M.M. Maximum Power Point Tracking of a Grid Connected PV Based Fuel Cell System Using Optimal Control Technique. *Sustainability* **2023**, *15*, 3980. [[CrossRef](#)]
15. Zheyuan, C.; Hammid, A.; Kareem, A.; Jiang, M.; Mohammed, M.; Kumar, N. A Rigid Cuckoo Search Algorithm for Solving Short-Term Hydrothermal Scheduling Problem. *Sustainability* **2021**, *13*, 4277. [[CrossRef](#)]
16. Liaquat, S.; Fakhar, M.S.; Kashif, S.A.R.; Rasool, A.; Saleem, O.; Padmanaban, S. Performance Analysis of APSO and Firefly Algorithm for Short Term Optimal Scheduling of Multi-Generation Hybrid Energy System. *IEEE Access* **2020**, *8*, 177549–177569. [[CrossRef](#)]
17. Zeng, X.; Hammid, A.T.; Kumar, N.M.; Subramaniam, U.; Almakhles, D.J. A grasshopper optimization algorithm for optimal short-term hydrothermal scheduling. *Energy Rep.* **2021**, *7*, 314–323. [[CrossRef](#)]
18. Hassan, T.U.; Alquthami, T.; Butt, S.E.; Tahir, M.F.; Mehmood, K. Short-term optimal scheduling of hydro-thermal power plants using artificial bee colony algorithm. *Energy Rep.* **2020**, *6*, 984–992. [[CrossRef](#)]
19. Azad, A.S.; Rahaman, S.A.; Watada, J.; Vasant, P.; Vintaned, J.A.G. Optimization of the hydropower energy generation using Meta-Heuristic approaches: A review. *Energy Rep.* **2020**, *6*, 2230–2248. [[CrossRef](#)]
20. Zhao, J.; Zhang, Y.; Liu, Z.; Hu, W.; Su, D. Distributed multi-objective day-ahead generation and HVDC transmission joint scheduling for two-area HVDC-linked power grids. *Int. J. Electr. Power Energy Syst.* **2021**, *134*, 107445. [[CrossRef](#)]
21. Nemati, M.; Braun, M.; Tenbohlen, S. Optimization of unit commitment and economic dispatch in microgrids based on genetic algorithm and mixed integer linear programming. *Appl. Energy* **2018**, *210*, 944–963. [[CrossRef](#)]
22. Bento, P.M.R.; Mariano, S.J.P.S.; Calado, M.R.A.; Ferreira, L.A.F.M. A Novel Lagrangian Multiplier Update Algorithm for Short-Term Hydro-Thermal Coordination. *Energies* **2020**, *13*, 6621. [[CrossRef](#)]
23. Ergun, H.; Dave, J.; Van Hertem, D.; Geth, F. Optimal Power Flow for AC–DC Grids: Formulation, Convex Relaxation, Linear Approximation, and Implementation. *IEEE Trans. Power Syst.* **2019**, *34*, 2980–2990. [[CrossRef](#)]
24. Castro, L.M.; González-Cabrera, N.; Guillen, D.; Tovar-Hernández, J.; Gutiérrez-Alcaraz, G. Efficient method for the optimal economic operation problem in point-to-point VSC-HVDC connected AC grids based on Lagrange multipliers. *Electr. Power Syst. Res.* **2020**, *187*, 106493. [[CrossRef](#)]
25. Nguyen, T.T.; Pham, L.H.; Mohammadi, F.; Kien, L.C. Optimal Scheduling of Large-Scale Wind-Hydro-Thermal Systems with Fixed-Head Short-Term Model. *Appl. Sci.* **2020**, *10*, 2964. [[CrossRef](#)]
26. Ahmad, A.; Kashif, S.A.R.; Nasir, A.; Rasool, A.; Liaquat, S.; Padmanaban, S.; Mihet-Popa, L. Controller Parameters Optimization for Multi-Terminal DC Power System Using Ant Colony Optimization. *IEEE Access* **2021**, *9*, 59910–59919. [[CrossRef](#)]
27. Gulzar, M.M.; Sibtain, D.; Ahmad, A.; Javed, I.; Murawwat, S.; Rasool, I.; Hayat, A. An Efficient Design of Adaptive Model Predictive Controller for Load Frequency Control in Hybrid Power System. *Int. Trans. Electr. Energy Syst.* **2022**, *2022*, 7894264. [[CrossRef](#)]
28. Baradar, M.; Ghandhari, M. A Multi-Option Uni Fi Ed Power Flow Approach for Hybrid AC/DC Grids Incorporating. *IEEE Trans. Power Syst.* **2013**, *28*, 2376–2383. [[CrossRef](#)]
29. Gonzalez-Torres, J.C.; Damm, G.; Costan, V.; Benchaib, A.; Lamnabhi-Lagarrigue, F. A Novel Distributed Supplementary Control of Multi-Terminal VSC-HVDC Grids for Rotor Angle Stability Enhancement of AC/DC Systems. *IEEE Trans. Power Syst.* **2020**, *36*, 623–634. [[CrossRef](#)]
30. Sibtain, D.; Gulzar, M.M.; Shahid, K.; Javed, I.; Murawwat, S.; Hussain, M.M. Stability Analysis and Design of Variable Step-Size P&O Algorithm Based on Fuzzy Robust Tracking of MPPT for Standalone/Grid Connected Power System. *Sustainability* **2022**, *14*, 8986. [[CrossRef](#)]
31. Cao, J.; Du, W.; Wang, H.F.; Member, S. An Improved Corrective Security Constrained OPF for Meshed AC/DC Grids with multi-terminal VSC-HVDC. *IEEE Trans. Power Syst.* **2015**, *31*, 485–495. [[CrossRef](#)]
32. Al-Sakkaf, S.; Kassas, M.; Khalid, M.; Abido, M.A. An Energy Management System for Residential Autonomous DC Microgrid Using Optimized Fuzzy Logic Controller Considering Economic Dispatch. *Energies* **2019**, *12*, 1457. [[CrossRef](#)]
33. Salman, U.; Khan, K.; Alismail, F.; Khalid, M. Techno-Economic Assessment and Operational Planning of Wind-Battery Distributed Renewable Generation System. *Sustainability* **2021**, *13*, 6776. [[CrossRef](#)]
34. Alhumaid, Y.; Khan, K.; Alismail, F.; Khalid, M. Multi-Input Nonlinear Programming Based Deterministic Optimization Framework for Evaluating Microgrids with Optimal Renewable-Storage Energy Mix. *Sustainability* **2021**, *13*, 5878. [[CrossRef](#)]
35. Khalid, M. Wind Power Economic Dispatch—Impact of Radial Basis Functional Networks and Battery Energy Storage. *IEEE Access* **2019**, *7*, 36819–36832. [[CrossRef](#)]
36. Khalid, M.; Ahmadi, A.; Savkin, A.V.; Agelidis, V.G. Minimizing the energy cost for microgrids integrated with renewable energy resources and conventional generation using controlled battery energy storage. *Renew. Energy* **2016**, *97*, 646–655. [[CrossRef](#)]
37. Gulzar, M.M.; Iqbal, A.; Sibtain, D.; Khalid, M. An Innovative Converterless Solar PV Control Strategy for a Grid Connected Hybrid PV/Wind/Fuel-Cell System Coupled with Battery Energy Storage. *IEEE Access* **2023**. [[CrossRef](#)]
38. Gulzar, M.M.; Sibtain, D.; Khalid, M. Cascaded Fractional Model Predictive Controller for Load Frequency Control in Multiarea Hybrid Renewable Energy System with Uncertainties. *Int. J. Energy Res.* **2023**. [[CrossRef](#)]

Disclaimer/Publisher’s Note: The statements, opinions and data contained in all publications are solely those of the individual author(s) and contributor(s) and not of MDPI and/or the editor(s). MDPI and/or the editor(s) disclaim responsibility for any injury to people or property resulting from any ideas, methods, instructions or products referred to in the content.